Extended Abstracts of the 2015 International Conference on Solid State Devices and Materials, Sapporo, 2015, pp712-713

Tolerance to UV-O_3 Exposure of CVD and Mechanically Exfoliated MoS_2 & Fabrication of Top-Gated CVD MoS_2 FETs

[1*]S. Kurabayashi and [1,2]K. Nagashio
[1]Department of Materials Engineering, The University of Tokyo
7-3-1 Hongo, Bunkyo-ku, Tokyo, 113-8656 Japan
[2]PRESTO-JST, Japan
*E-mail: kurabayashi@ncd.t.u-tokyo.ac.jp

In this work, well-separated triangle MoS_2 crystals were synthesized at large area on the SiO_2/Si substrate by CVD. The ozone exposure experiment indicated that the tolerance to UV-O_3 for exfoliated MoS_2 is higher than that for CVD MoS_2. The narrower PL peak for CVD MoS_2 seems not to be due to the low defect density, but due to the strain induced during CVD. This is supported by the Raman data. Finally, we demonstrated the Al_2O_3 top gate FET with negligible leakage currents.

1. Introduction

The perspective to overcome the short channel effect based on the scaling length [1] attracts great attention to 2D layered MoS_2 semiconductors, due to their rigidly-controllable few atomic thickness. It's important to synthesize high quality MoS_2, because the quality of bulk MoS_2 is not high in contrast to Kish graphite. The chemical vapor deposition (CVD) using S and MoO_3 precursors has been the primary approach for MoS_2 synthesis [2]. The photoluminescence (PL) peak for CVD MoS_2 is narrower than that for mechanically-exfoliated (ME) one [3], which generally suggests that the films are typically of high quality comparable to ME. The mobility for CVD MoS_2, however, is always lower than that for ME MoS_2 [4]. This discrepancy results from the unavailability of quantitative method to evaluate the amount of defects in MoS_2, in contrast with Raman D band intensity in graphene. Although the tolerance of MoS_2 films to UV-O_3 provides the information on defects, no comparison of ME and CVD MoS_2 has been reported.

In this study, we first investigate the appropriate substrate position during the CVD growth. Then, the tolerance to UV-O_3 for CVD and ME MoS_2 are investigated to evaluate the crystallinity. Finally, to characterize the electrical transport properties, the top gate FET was fabricated using CVD-MoS_2.

2. Chemical vapor deposition

Fig. 1a shows a schematic illustration of growth tube furnace where MoO_3 and S boats are located at the center and the upper stream region of N_2 gas flow, respectively. MoO_3 was heated to 600℃ or 700℃. Three set of substrates (A1~3 or B1~3) can be placed for one growth run. In case of B1~3, the substrate holder was used to adjust the height (not shown in the figure).

The growth of MoS_2 was observed mainly at A2 and B2, not at other positions. **Figures 1b & c** show the optical images at A2 and B2, respectively. At both positions, typical triangle shape of MoS_2 is observed. From the viewpoint of the device fabrication, B2 is more suitable than A2, because MoS_2 triangles are completely separated and the growth area is roughly 10 times larger. The maximum size obtained recently is ~100 μm in length (inset), which is largest reported so far in the literatures. At A2, Mo content on the substrate is large enough because of the short distance between MoO_3 and substrate, resulting in the continuous film of MoS_2. On the other hand, at B2, reduced Mo content on the substrate leads to separated triangles, but the higher growth temperature is required (700°C for B2, 600°C for A2). Based on these discussion, the control of Mo content on the substrate could be the main growth factor.

Figure 2 shows (a) PL spectra and (b) Raman data for CVD and ME MoS_2. The full width at half maximum of PL spectrum for CVD MoS_2 (~0.06eV) was lower than

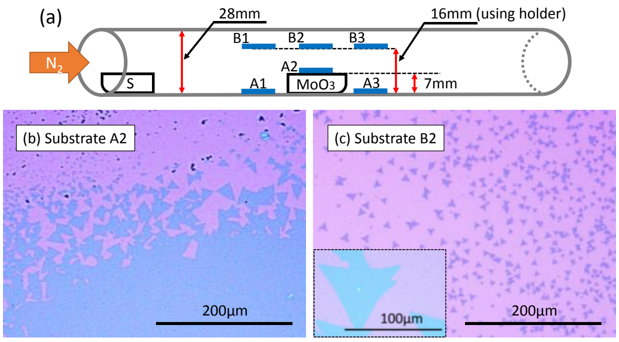

Fig. 1 (a) Schematic illustration of growth tube furnace, and optical images for MoS_2 triangles observed at (b) A2 at 600°C and (c) B2 at 700°C, respectively.

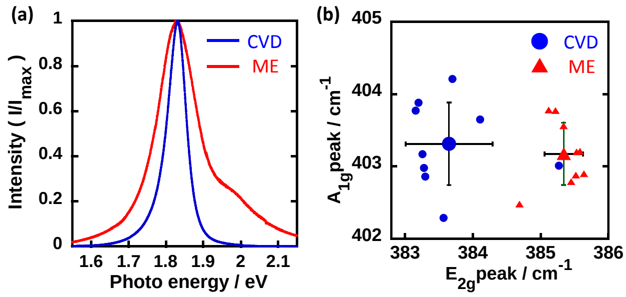

Fig. 2 (a) PL spectra for CVD and ME MoS_2. The vertical axis is normalized by maximum intensity. (b) Raman map for CVD and ME MoS_2.

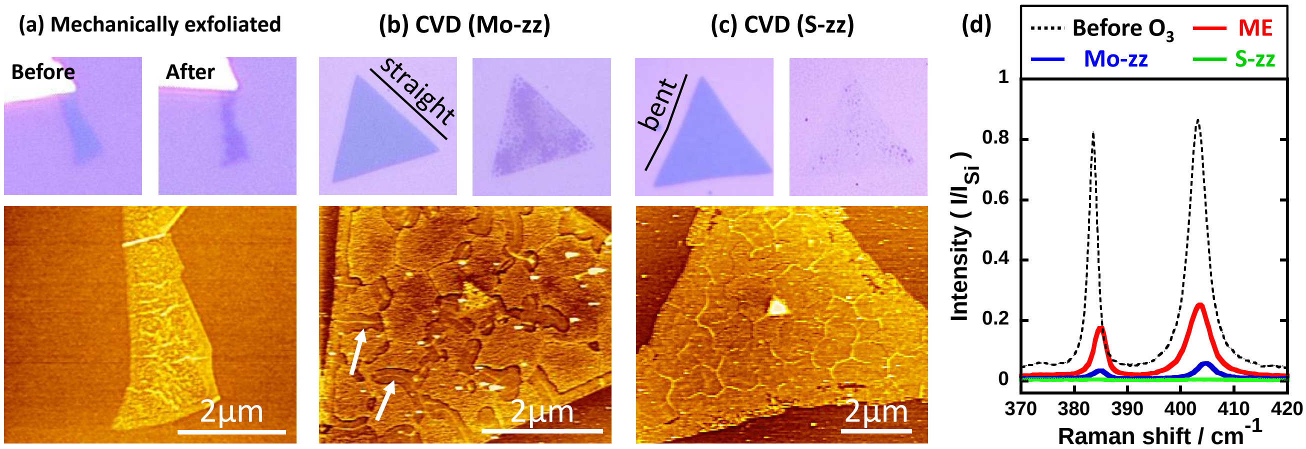

Fig. 3 (a)~(c) Optical images before and after UV-O_3 exposure. Mo-zz edge is straight, while S-zz edge is bent. AFM images after UV-O_3 exposure and change of appearance in optical microscope (d) Raman peaks for three samples after UV-O_3 exposure. The dotted line indicates the Raman peaks for non UV-O_3 treated MoS_2 as a standard. All the data was normalized by the intensity of Si.

that for ME one (~0.1eV), which is consistent with the previous report [3]. E_{2g} peak for CVD MoS_2 is red-shifted from that for ME MoS_2, suggesting that in-plane vibration is weakened. It is expected that the amount of strain due to the interaction with the substrate is different.

3. Tolerance to UV-O_3 for CVD and ME MoS_2

In order to evaluate the crystallinity of CVD and ME MoS_2, the tolerance of MoS_2 to the UV-O_3 was studied. According to the literature [5], CVD MoS_2 can be categorized into 2 groups; Mo-zigzag edge (Mo-zz) and S-zigzag edge (S-zz). The Mo-zz edge is shaper and linear than the S-zz one. Mo-zz is generally found at the downstream of N_2 gas flow (Mo-rich area) because Mo-zz is likely to grow at Mo-rich area. This difference can be clearly seen in **Fig. 3**. Each MoS_2 was exposed to UV-O_3 (~25ppm) at 150°C for 5 min.

After UV-O_3 exposure, the optical contrast for ME MoS_2 became dark purple, while the morphology is not changed so much in AFM image. Raman peak intensity is reduced. Mo-zz MoS_2 partially become spotted dark purple; in fact, the some part of top S layer seems to be etched away in AFM image. At the etched region, the line can be seen, as shown by arrows in AFM image. Raman peak intensity was largely decreased. On the other hand, the whole surface of S-zz MoS_2 became light-colored. It is difficult to see it by optical image. However, in AFM image, S-zz MoS_2 still exists but top S layer were totally etched away, and lines are observed throughout the sample. In this case, Raman peak disappeared. This means that the etching rate of top S-layer is much faster for S-zz MoS_2.

Based on these results, the order of tolerance to UV-O_3 is ME > CVD Mo-zz > CVD S-zz. In other words, the defect density for CVD MoS_2 is larger than that for ME MoS_2. The narrower FWHM in PL for CVD MoS_2 in **Fig. 2a** is not due to the low defect density, but due to the strain induced in the films during the CVD growth, which can be supported by the Raman data in **Fig. 2b**.

4. ALD-Al_2O_3 top-gate FET

Mo-zz MoS_2 was selected for the device. The Y metal with 1.5 nm was deposited on MoS_2 channel and then oxidized at 200°C. Subsequently, ~25 nm Al_2O_3 was deposited by atomic layer deposition (ALD) at 200°C using trimethylaluminum and water. Finally, Al was deposited as a top gate electrode. **Figure 4** shows (a) schematic illustration and (b) optical image for this device. Transport characteristics are shown in **Fig. 4c**. Because of intrinsic band gap (~1.85eV), clear transfer curve is obtained. The gate leakage current is 5 orders lower than drain current, suggesting that the top gate insulator is quite good quality.

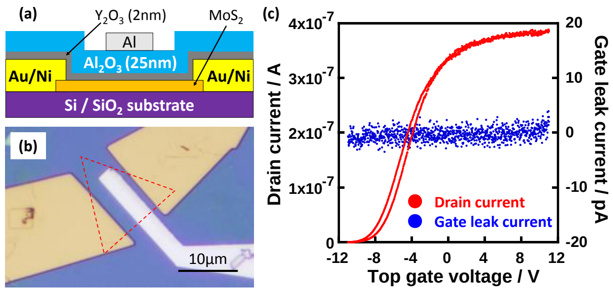

Fig. 4 Schematic illustration (a) and optical image (b) optical image of the device. (c) Drain and leakage currents as a function of top gate voltage.

5. Conclusions

The order of tolerance to O_3 was ME > CVD Mo-zz > CVD S-zz, suggesting that the defect density for CVD MoS_2 is larger than that for ME MoS_2. The narrower FWHM in PL for CVD MoS_2 is not due to the low defect density, but due to the strain induced in the films during the CVD growth. The further improvement of crystalline quality is required for device applications.

Acknowledgements: This work was partly supported by a Grant-in-Aid for Scientific Research from the MEXT in JAPAN.

Reference: [1] I. Ferain, *et al.*, *Nature* 2011, **479**, 310. [2] A. M. van der Zande, *et al.*, *Nature Mater*. 2013, **12**, 554. [3] M. Amani, *et al.*, *Appl. Phys. Lett*. 2014, **104**, 203506. [4] H. Liu, *et al.*, *Nano lett*. 2013, **13**, 2640. [5] L. Byskov, *et al.*, *Catal. Lett*. 2000, **64**, 95.